



Published in final edited form as:

J Am Chem Soc. 2010 February 3; 132(4): 1230. doi:10.1021/ja909947a.

The Structural Basis of *Cryptosporidium*-Specific IMP Dehydrogenase Inhibitor Selectivity

Iain S. MacPherson[†], Sivapriya Kirubakaran[†], Suresh Kumar Gorla[†], Thomas V. Riera[‡], J. Alejandro D'Aquino[‡], Minjia Zhang[†], Gregory D. Cuny[§], and Lizbeth Hedstrom^{†,¶}

[†]Department of Biology, Brandeis University, MS009, 415 South St. Waltham, MA 02454

[‡]Department of Biochemistry, Brandeis University, MS009, 415 South St. Waltham, MA 02454

[¶]Department of Chemistry, Brandeis University, MS009, 415 South St. Waltham, MA 02454

[§]Laboratory for Drug Discovery in Neurodegeneration, Brigham & Women's Hospital, Harvard Medical School, 65 Landsdowne Street, Cambridge, MA 02139

Cryptosporidium spp. are a major cause of the “vicious cycle” of diarrhea and malnutrition in the developing world and a potential bioterrorism agent ^{1,2}. This disease is prolonged and life-threatening in immuno-compromised patients. Currently no effective therapy exists for *Cryptosporidium* infections. The parasite obtains guanine nucleotides via a streamlined pathway that requires inosine 5'-monophosphate dehydrogenase (IMPDH) ³⁻⁵. Curiously, the gene encoding *Cp*IMPDH appears to have been obtained from a bacteria via lateral gene transfer ^{6,7}; we have exploited this unexpected divergence of parasite and host enzymes to identify *Cp*IMPDH-specific inhibitors in a high throughput screen ⁸. Here we report x-ray crystal structures of *Cp*IMPDH that explain the selectivity of one inhibitor series and use this information to design more potent and selective analogs.

Recombinant *Cp*IMPDH was purified as described previously ⁹ and crystallized using the hanging drop vapor diffusion method. Protein solution (4 mg/mL IMPDH, 50 mM Tris-HCl, pH 7.5, 150 mM KCl, 5% glycerol and 2 mM DTT) was mixed with well solution (34% PEG 4000, 25 mM sodium acetate and 100 mM Tris-HCl, pH 8.5) in a 1:1 ratio. Data were collected from a single crystal at 100K at beamline 8-BM at Advanced Photon Source (Argonne National Laboratory, Argonne, IL). The crystals had the symmetry of space group P2₁2₁2. The asymmetric unit contains one tetramer, which is the active form of IMPDH¹². The structure was solved to 3.2 Å resolution ($R = 27\%$, $R_{free} = 33\%$) by molecular replacement using the structure of IMPDH from *Borrelia burgdorferi* (PDB accession 1EEP10) as a search model¹¹. Only 301 of 400 residues are visible in the most structured monomer; the disordered regions include catalytically important segments 214-222, 299-333 and 380-400 as well as residues 92-122, which are not required for enzymatic activity ¹². Unfortunately, we were unable to improve this crystal form. This structure has been deposited in the PDB (3FFS).

To facilitate crystallization, residues 90-134 were replaced with SerGlyGly¹¹; this modification has no effect on enzymatic activity (Figure S1). A crystallization screen was performed in the presence of IMP and various inhibitors that emerged from initial evaluation of the SAR. Compound **C64** was a particularly attractive candidate for crystallization because of its improved potency relative to the parent compound **C** and the presence of a bromine atom

hedstrom@brandeis.edu.

Supporting Information Available: Methods, crystallographic data table, spectra, chromatograms and complete Refs. 4 & 5 (PDF). This material is available free of charge via the Internet at <http://pubs.acs.org>.

which would allow the two aromatic groups to be easily distinguished (Table 1). Crystals were obtained in the presence of saturating concentrations of inhibitor **C64** (20 μ M), IMP (1 mM), 100 mM sodium acetate, pH 4.6, 20 mM CaCl₂ and 30% MPD under oil. These crystals had the symmetry of space group $P2_1$ with two tetramers in the asymmetric unit. Data were collected at a wavelength of 0.9194 Å, enabling the simultaneous collection of bromine k-edge anomalous dispersion data. The structure was solved by molecular replacement to 2.8 Å resolution using the native *Cp*IMPDPH structure as the starting model ($R = 26.6\%$, $R_{free} = 22.4\%$).

While the overall structure of the E•IMP•**C64** complex is similar to that of the unliganded enzyme, several additional residues are observed. Residues 214-226, which include the catalytic Cys219, are observed in most of the monomers, as are parts of the active site flap (residues 302-330) containing the characteristic ArgTyr motif¹². Lastly, the SerGlyGly linker is visible in all monomers. Electron density for IMP is observed in all eight monomers. Monomers B, D and H contained extra electron density near IMP (Figure 1). Bromine k-edge anomalous dispersion maps allowed the unambiguous assignment of the bromine atom in **C64** in all three monomers. The rest of **C64** was modeled into the remaining electron density; similar conformations of **C64** are obtained in all three monomers. This structure has been deposited in the PDB (3KHJ).

Surprisingly, **C64** binds in an unprecedented fashion. Inhibitors of human IMPDH2 such as mycophenolic acid and merimepodib bind in the nicotinamide subsite, stacking against the purine ring of IMP in a parallel fashion, and extend either into the NAD site or into a pocket adjacent the active site but within the same monomer¹²⁻¹⁴. In contrast, the thiazole ring of **C64** stacks against the purine ring of IMP perpendicularly, and the remainder of **C64** extends across the subunit interface into a pocket in the adjacent monomer, where the bromoaniline moiety interacts with Tyr358' (where ' denotes a residue from the adjacent subunit; Figure 2). This residue forms a hydrogen bonding network involving Glu329, Ser354, Thr221 and possibly the amide nitrogen of **C64** (Figure 2). Ser22', Pro26', Ala165, Gly357' form the remainder of the inhibitor binding pocket. With the exception of Thr221, all of these residues are different in human IMPDHs (Figure 2). Thus these interactions account for the selectivity of **C64** for *Cp*IMPDPH over human IMPDHs.

The structure also revealed the presence of a cavity adjacent to the bromoaniline moiety (Figure 1), which suggested that more potent inhibitors might be created by increasing the bulk of this substituent. Additional benzimidazole based inhibitors were prepared by condensing *o*-phenylenediamine **1** with thiazole carboxaldehydes **2** in the presence of the oxidizing reagent sodium metabisulfite **3** (Scheme 1)¹⁵. The resulting 2-substituted benzimidazoles **4** were then coupled with different bromoacetyl amides **5** under mild basic conditions to give the new analogs **6** (Table 1).

The *Cp*IMPDPH inhibitory activity of the compounds was assessed by monitoring the production of NADH by fluorescence (Table 1)¹⁶. Replacing the *p*-MeO of the parent compound **C** with Cl or Br increased potency by 10-fold (**C10**) and 20-fold (**C14**), respectively, as has been similarly observed with another inhibitor series.¹⁶ To fill the cavity observed in the crystal structure, the *para*-substituted aniline group was replaced with 3,4-dichloroaniline (**C86**) or 2-naphthylamine (**C90**); the addition of a second Cl improved potency by a factor of 2, while fusing an additional aromatic ring increased potency by a factor of 8. Similar trends were observed when the thiazole ring was attached at the 2-position (**C61**, **C64**, **C84** and **C90**). None of the compounds displayed significant inhibitory activity against human IMPDH2. The best *Cp*IMPDPH inhibitor, **C90**, has an IC₅₀ = 7.4 nM with selectivity >10³ for the parasite enzyme.

In conclusion, the crystal structure of *Cp*IMPDPH reveals the structural basis of inhibitor selectivity and a strategy for further optimization. This information was used to design more potent and selective inhibitors of *Cp*IMPDPH that are potential lead compounds for the treatment of cryptosporidiosis.

Supplementary Material

Refer to Web version on PubMed Central for supplementary material.

Acknowledgments

This work was supported by funding from NIH/NIAID (U01AI075466) to LH. GDC thanks NERCE/BEID, the Harvard NeuroDiscovery Center and the Partners Center for Drug Discovery for financial support. Initial crystal screening was performed at the Hauptman Woodward Institute. We thank Jennifer Lu for assistance in obtaining crystals of the unliganded complex, Kene Piasta for data collection and our colleague Gregory Petsko for advice and comments on the manuscript.

References

1. Fayer R. *Veterinary Parasitology* 2004;126:37–56. [PubMed: 15567578]
2. Huang DB, White AC. *Gastroenterol Clin North Am* 2006;35:291–314. viii. [PubMed: 16880067]
3. Striepen B, Pruijssers AJ, Huang J, Li C, Gubbels MJ, Umejiego NN, Hedstrom L, Kissinger JC. *Proc Natl Acad Sci U S A* 2004;101:3154–9. [PubMed: 14973196]
4. Abrahamsen MS, et al. *Science* 2004;304:441–445. [PubMed: 15044751]
5. Xu P, et al. *Nature* 2004;431:1107–1112. [PubMed: 15510150]
6. Striepen B, White MW, Li C, Guerini MN, Malik SB, Logsdon JM Jr, Liu C, Abrahamsen MS. *Proc Natl Acad Sci U S A* 2002;99:6304–6309. [PubMed: 11959921]
7. Umejiego NN, Li C, Riera T, Hedstrom L, Striepen B. *J Biol Chem* 2004;279:40320–40327. [PubMed: 15269207]
8. Umejiego NN, Gollapalli D, Sharling L, Volftsun A, Lu J, Benjamin NN, Stroupe AH, Riera TV, Striepen B, Hedstrom L. *Chem Biol* 2008;15:70–77. [PubMed: 18215774]
9. Riera TV, Wang W, Josephine HR, Hedstrom L. *Biochemistry* 2008;47:8689–96. [PubMed: 18642884]
10. McMillan FM, Cahoon M, White A, Hedstrom L, Petsko GA, Ringe D. *Biochemistry* 2000;39:4533–4542. [PubMed: 10758003]
11. See supplementary information for details.
12. Hedstrom L. *Chem. Rev* 2009;109:2903–2928. [PubMed: 19480389]
13. Sintchak MD, Fleming MA, Futer O, Raybuck SA, Chambers SP, Caron PR, Murcko M, Wilson KP. *Cell* 1996;85:921–930. [PubMed: 8681386]
14. Sintchak MD, Nimmegern E. *Immunopharmacology* 2000;47:163–184. [PubMed: 10878288]
15. Yang D, Fokas D, Li J, Yu L, Baldino CM. *Synthesis* 2005:47–56.
16. Maurya SK, Gollapalli DR, Kirubakaran S, Zhang M, Johnson CR, Benjamin NN, Hedstrom L, Cuny GD. *J Med Chem* 2009;52:4623–30. [PubMed: 19624136]

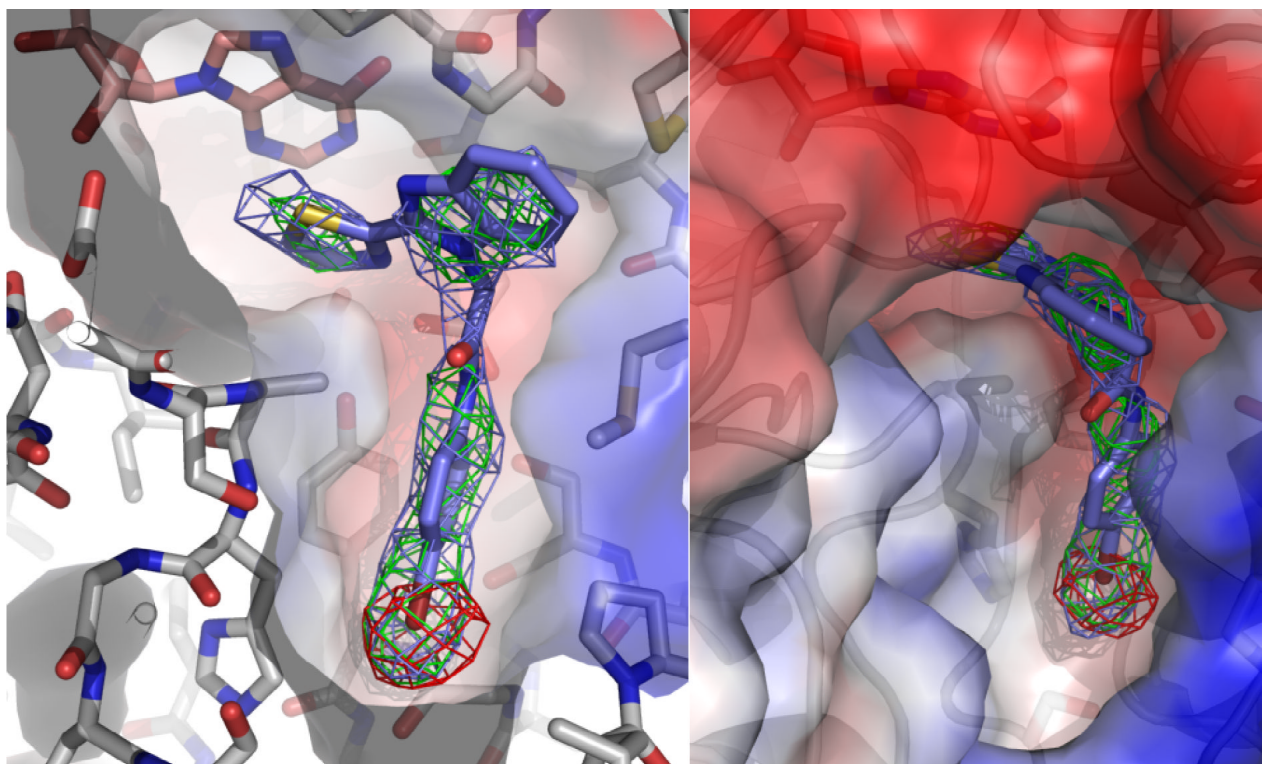


Figure 1.

Co-crystallized structure of *CpIMPDH* (light gray) with IMP (salmon) and **C64** (slate) shown from two different perspectives. The electron density map prior to **C64** modeling with coefficients $2F_o-F_c$ is contoured to 1σ and shown as a slate cage. The electron density map prior to **C64** modeling with coefficients F_o-F_c is contoured to 3σ and shown as a green cage. Bromine K-edge peak anomalous dispersion map is contoured to 4σ and shown as a red cage. The red and blue surfaces denote regions of negative and positive electrostatic potential, respectively.

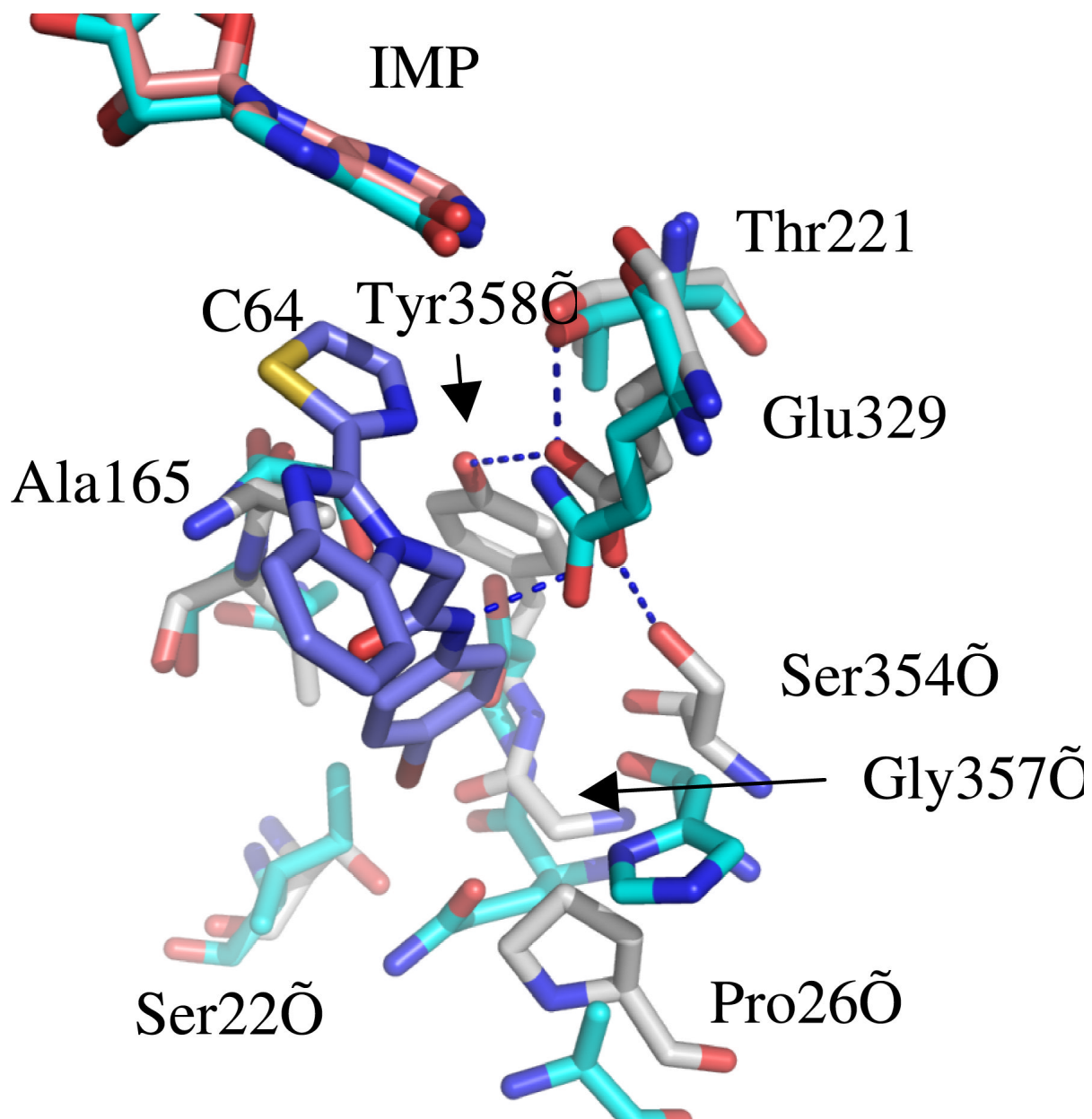
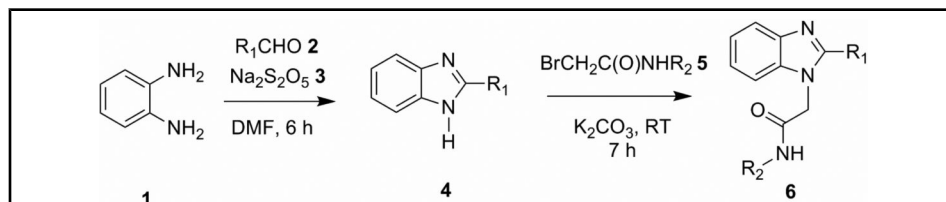


Figure 2.
The C64 binding pocket of *Cp*IMPDH (green) superposed with human IMPDH2 (cyan).
*Cp*IMPDH residues are labeled.

Table 1

Inhibition of CpIMPDPH and hIMPDPH2.



Scheme 1. Synthesis of inhibitors.

Cmpd	R ₁	R ₂	IC ₅₀ (nM)	
			CpIMPDPH	hIMPDPH2
C		4-OMePh	1200 ± 200 ^a	≥200,000 ^{a,b}
C10		4-ClPh	120 ± 40	≥20,000 ^c
C14		4-BrPh	60 ± 30	≥20,000 ^c
C86		2,3-Di-ClPh	30 ± 10	≥40,000 ^d
C90		2-Naph	7 ± 4	≥40,000 ^d
C61		4-ClPh	30 ± 10	≥40,000 ^d
C64		4-BrPh	28 ± 9	≥40,000 ^d
C84		2,3-di-ClPh	18 ± 5	≥8,000 ^e
C97		2-Naph	8 ± 3	≥40,000 ^d

^a values from ⁸.^b ≤20% inhibition at 50 μM^c ≤20% inhibition at 5 μM^d ≤ 10% inhibition at 5 μM^e ≤ 20% inhibition observed at 2 μM.